Chemical Physics Letters 555 (2013) 154–158

Contents lists available at SciVerse ScienceDirect

Chemical Physics Letters

journal homepage: www.elsevier.com/locate/cplett

Controllable growth of ZnO mesocrystals using a facile electrochemical approach

Tian Li, Zijun Cao, Hongjun You, Minwei Xu, Xiaoping Song, Jixiang Fang *

School of Science, MOE Key Laboratory for Nonequilibrium Synthesis and Modulation of Condensed Matter, Xi'an Jiaotong University, Shann Xi 710049, People's Republic of China

ARTICLE INFO

Article history:
Received 6 June 2012
In final form 17 October 2012
Available online 27 October 2012

ABSTRACT

We developed an electrochemical approach for the synthesis of ZnO mesocrystals with controlled aspect ratios. The ZnO mesocrystals performed 3 stages including nucleation, growth and subsequently self-assembly into a 3D architecture during the growth process. A nonclassical mechanism 'oriented attachment (OA)' is responsible for the formation of wurtzite ZnO mesocrystals. Based on the understanding for the growth mechanism, various ZnO mesocrystals with different aspect ratios was synthesized by controlling the current density of deposition. Their cathodoluminescent (CL) spectra showed an enhanced increase with the decrease of aspect ratios (length to diameter). This Letter is potentially helpful for researchers to understand the aggregation-driven formation of complex high-order structured materials.

1. Introduction

Mesocrystals, a new class of crystals, have attracted considerable research attention in recent years because of their unique structural characteristics including rough surface, high internal porosity, small size of building block, high crystalline defects as well as complex morphology [1]. These nonclassical crystals always have 3-dimensional (3D) superstructures composed of nanocrystal building blocks assembled in a crystallographically oriented attachment (OA) manner, which was first deduced by Cölfen and his co-workers from biomineralization processes [2]. Up to now, much attentions has been called up to the synthesis of mesostructures, most examples known are arguably oxides or carbonates [3–6]. However, several fundamental aspects about mesocrystals remain largely unexplored: firstly, what is the underlying growth mechanism during the highly ordered mesoscale assembly; secondly, how to develop the controllability of these unique growth modes when they are used to artificially synthesize advanced functional materials; thirdly, how to improve the possibility of exploiting more novel properties from the unique mesostructures. In this regard it seems to open the way to tailor the structures and hence all structure-dependent properties of mesocrystals [7].

As a wide-gap (3.37 eV) II–VI semiconductor, ZnO material is a promising candidate for a number of applications, such as the ultraviolet devices, catalysis, piezoelectrics, and gas sensors [8–11]. It is well accepted that the morphology and size of ZnO are important elements in determining its physical and chemical properties for above applications. Hence, many recent efforts have been spurred in researches on the synthesis of ZnO nanostructures with diverse morphologies such as nanorods, hollow spheres, flower-like, tower-like and flim structures [12–16]. However, there are only a few reports which focus on the synthesis of ZnO mesostructure [17]. Very recently, Distaso et al. reported a synthesis of ZnO mesocrystals by a solvothermal route and their structures are well controlled by the polymer chain length [18]. It is a representative research on the mesocrystals synthesis and the fine-tuning of the optical properties of ZnO mesocrystals.

In this Letter, we report an electrochemical route to synthesize rice-like ZnO mesocrystals at a low-temperature (80 °C). Electrodeposition in the study is greatly simplified. More facile selections of great scientific and technological interest have been brought to the experiments, including the simplification of the electrode system and the optimization of the electrolyte even giving up using any surfactant. As the unusual growth mode for silver observed by Fang et al. [19] another non-classical crystalline growth mode for ZnO particles is given here. The as-synthesized ZnO nanorices are found to be built up from the self-assembly of ZnO nanoparticles, which share a similar crystallographic orientation. The structural and morphological evolution of ZnO mesocrystals are deeply studies based on the oriented attachment (OA) mechanism. Additionally, we study the close relationship between the current density of deposition and optical properties with the cathodoluminescent (CL) measurement. On the other hands, no obvious UV emission is observed in the CL spectra, which indicates the presence of larger density of defects in the interior of ZnO particles.

2. Experimental section

The synthesis of ZnO mesocrystals was carried out in a steady environment by use of a potentiostat. Two pieces of zinc foils (1 cm × 0.5 cm in size, Alfa, 99.99%) were used as the working electrode and counter electrode separately. The distance between the two electrodes was kept at 1.5 cm. The electrolyte was an aqueous

* Corresponding author.
E-mail address: jxfang@mail.xjtu.edu.cn (J. Fang).

0009-2614/$ - see front matter © 2012 Elsevier B.V. All rights reserved.
http://dx.doi.org/10.1016/j.cplett.2012.10.046

solution of KCl (10 mmol, analytical grade and used as received without further purification). The ZnO mesocrystals were electrochemically grown at a constant voltage of 30 V for 7 min at 80 °C. The products obtained in solution were harvested by centrifugation (3000 rpm for 5 min) and dried at 60 °C. To investigate the role of preparation conditions in determining the mesocrystal morphologies, the reaction potentials and the KCl concentrations were varied while the essential conditions were kept the same.

The structure and morphology of the products were characterized with X-ray powder diffraction (XRD, Bruke D8-Advance, Cu-Kα, λ = 0.15406 nm), field-emission scanning electron microscopy (FE-SEM, JEOL JSM-7000F) and transmission electron microscopy (TEM, JEOL JEM-2100). The CL measurements were carried out in a vacuum chamber ($<10^{-3}$ Pa), which was pumped by a rotary and turbo molecular pump. In the vacuum chamber, the phosphors were excited by an electron beam at an accelerating voltage range of 1–5 kV with different bombardment current density. The CL spectra were measured with a fiber-optic coupled spectrometer (SL-300).

3. Results and discussion

Figure 1 shows the SEM images and corresponding XRD patterns of the as-prepared ZnO products. The low-magnified image in Figure 1a reveals that the mesocrystals can be produced in large-scale with a uniform 3D rice-like morphology composed by two symmetrical cones (the inset of Figure 1a). Statistical result indicate that the rice-like ZnO particles have an average length of 720 nm and a mean diameter of 300 nm and their aspect ratio (length/diameter) is about 2.4. More detailed characteristics are revealed by the high-magnified SEM image in Figure 1b. It can be seen that there is a joint boundary perpendicular to the length of the particles, which divides the particles into two sides. The corresponding XRD pattern is presented in Figure 1c, which reveals that all diffraction peaks of the product are in good agreement with the wurtzite ZnO (JCPDS 36-1451). No impurity peaks are detected. The relative sharp peaks in the XRD pattern confirm that the products crystallize in a pure hexagonal wurtzite structure. Interestingly, it is found that ZnO particles are composed of many small particles (the inset of Figure 1c). The assembly of the nanoparticles makes the ZnO mesocrystals exhibit rough surface, which reveals a nonclassical crystallization process.

To gain further insights on this unique nonclassical growth behavior, the obtained ZnO nanorices were structurally characterized by TEM. Figure 2a displays TEM images of the rice-like ZnO particles which agree well with the SEM results. The high-magnified SEM image of single nanorice is shown in Figure 2a, from which the orderly accumulation of ZnO nanoparticles could be observed. The SAED pattern (the inset of Figure 2b) shows the individual diffraction spots, demonstrating the single crystal nature for the rice-like ZnO mesocrystal. Moreover, the HRTEM image in Figure 2c originated from the surface of a rice-like ZnO particle shows a typical structure of mesocrystal. The parallelism of the lattice-fringes is indicated by arrows, which shows that each attached nanoparticle shares the same crystallographic orientation (like a single crystal). Hence, it can be concluded that the primary particles are orderly assembled together to form the rice-like mesocrystal.

The possible reaction process for the ZnO mesocrystals could be described by the formulas as follows:

$$\text{Anode}: Zn(s) \rightarrow Zn^{2+}(aq) + 2e^- \quad (1)$$

$$\text{Cathode}: 2H^+(aq) + 2e^- \rightarrow H_2 \uparrow \quad (2)$$

$$\text{Solution}: Zn^{2+}(aq) + 2OH^-(aq) \rightarrow ZnO(s) + H_2O \quad (3)$$

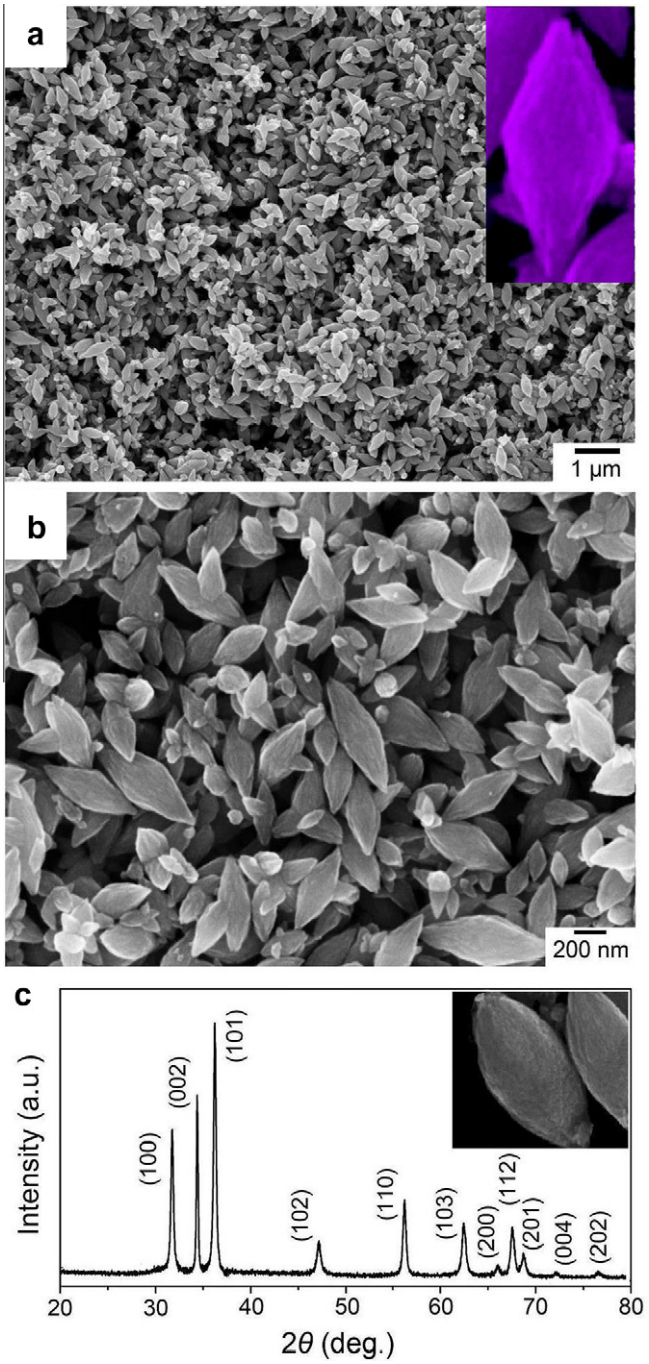

Figure 1. Morphological and structural characterizations of the rice-like ZnO particles obtained in 10 mmol/L KCl at 30 V (the current density is 750 mA/cm^2): (a) low-magnification SEM image, (b) high-magnification SEM image, (c) XRD pattern. The insert of (c) is high-magnification SEM image of ZnO particle surface.

Firstly, Zn^{2+} was formed in the solution due to the anodization of the zinc foil. Meanwhile, the release of H_2 could be observed at the cathode surface. Then, the Zn^{2+} combined with OH^- to form $Zn(OH)_2$. In fact, $Zn(OH)_2$ was not stable at high temperatures and tended to break down to ZnO and H_2O. Finally, the obtained ZnO nanocrystals were self-assembled with each other to form the ZnO mesocrystal.

To better understand the formation of rice-like ZnO mesocrystals, SEM images of ZnO particles obtained at different reaction times were characterized and presented in Figure 3. At the very early stages of the reaction (2–3 s), as Figure 3a reveals, the ZnO

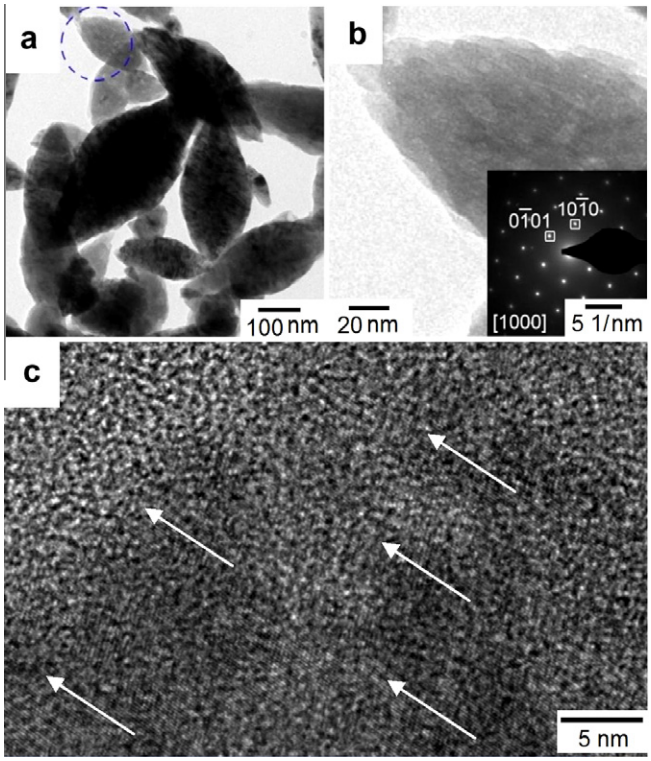

Figure 2. (a) Low-magnification TEM image of rice-like ZnO mesocrystals obtained in 10 mmol/L KCl at 30 V, (b) high-magnification TEM image of a rice-like from circled area in (a) and the correlated SAED pattern (inset), (c) representative HRTEM image at the tip of a rice-like ZnO particle.

cones were structurally and energetically favorable to form under the present preparation condition. Such structures likely formed through aggregation of discrete ZnO nanoparticles. Many unformed cones consist of large number of approximate ellipsoid nanoparticles can be seen, which reveals the growth process of cone structures. Following, when the reaction proceeded to ~10 s, two of ZnO cones began to combine regularly due to the high surface energy. The above two stages can be proved by the obvious gaps as marked by the arrows in Figure 3b. With longer reaction times (1 min), twin-cone structures formed by making up the gap, resulting in the integrated rice-like ZnO particles with rough surface. Careful examination of the SEM images from these later stages of reaction (5 min) reveals the smooth process of rice-like ZnO particles. The transient process at this special stage can be explained by the 'Ostwald ripening' (OR) mechanism, which has been widely proposed for the growth of ZnO [20–21]. Driven by surface energy reduction of ZnO particles, OR prefers to remove the irregularities arising from oriented aggregation and hence tends to yield rounded and smooth particles [7]. At the expense of small particles, ZnO grains continue to grow up and this growth process can be called coarsening, during which, two adjacent building units fuse together and the gaps between them decreases. As a result, the whole particle surface becomes smooth. Meanwhile, the grain size in Figure 3d becomes larger than that in Figure 3c.

From the above description of crystal morphology and growth process, it was evidently seen that the self-assembly of primary ZnO nanocrystals was in a crystallographically oriented manner to form the ZnO mesocones. This delicate assembly process is termed 'oriented attachment' (OA) and is widely documented in literatures concerning the formation of ZnO mesocrystals. Till now, a variety of ZnO mesocrystals have been developed, including mesoporous ZnO film [22] and mesostructure ZnO particles with irregular shape [23]. In our study, mesostructure ZnO with a rice-like shape were obtained. For the present experiment, the current density served as the driving force of the assembly process to facilitate formation of ZnO mesocrystals. Accordingly, a plausible formation mechanism for the rice-like ZnO mesocrystals was proposed and schematically illustrated in Figure 4. ZnO nanoparticles were the origin of the crystal growth and self-assemble along the identical direction serving as the building blocks. Subsequently, isotropically shaped primary nanocrystals were generated under the drive of the reaction current. A detailed and persuasive forming process of ZnO mesocones has been detailedly and vividly introduced by Dong et al. [24]. For a single cone, the round-bottom was firstly formed and then served as the base for the further growth along the preferred growth direction. Here, [0001] is the

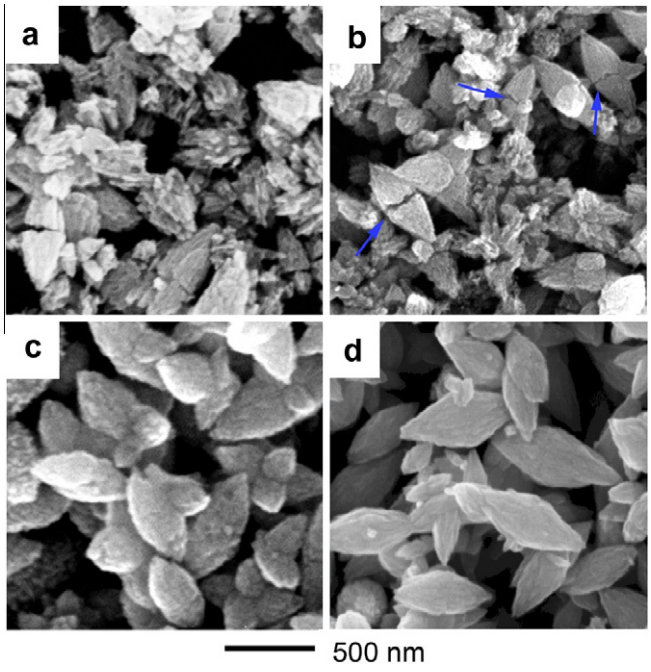

Figure 3. SEM images of the rice-like ZnO particles sampled at different reaction times (approximate): (a) 2–3 s, (b) ~10 s, (c) 1 min, and (d) 5 min. The arrow indicates the combination of two cones.

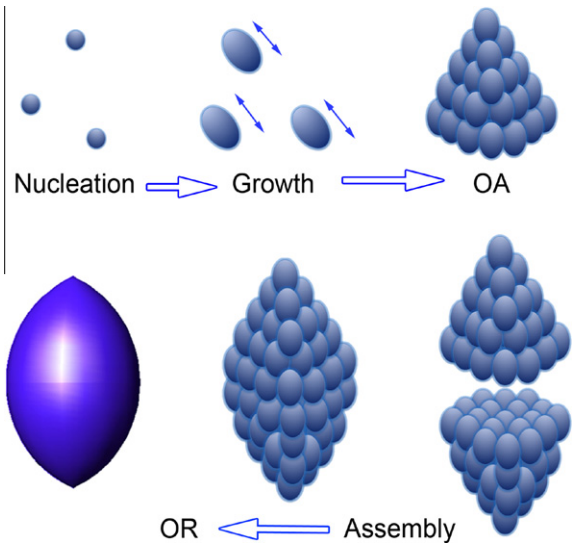

Figure 4. Schematic illustration for the formation of rice-like ZnO mesocrystals.

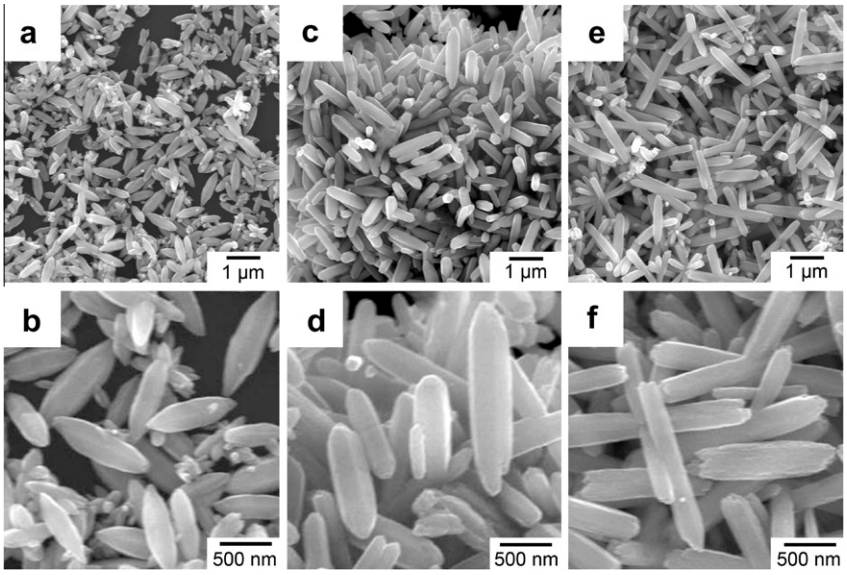

Figure 5. SEM images of ZnO mesocrystals obtained with different current densities: (a and b) 125; (c and d) 51.7; (e and f) 20 mA/cm^2. The corresponding voltages were 30, 5, and 1 V, respectively. The KCl concentration was kept at 1 mmol/L and the reaction times were 7 min.

preferred growth direction (*c*-axis) of ZnO because of the substantially largest surface energy of the (0001) plane. However, in the presence of a certain current condition, the growths along the minor axes of the anisotropic particles were not negligible, which would lead to an uneven, multi-dimensional growth of ZnO and the finally induced cone-like architectures. This phenomenon implies a transition of crystal growth habit from classical anisotropic crystal growth to nonclassical OA process depending on the current density. Two single cones with opposite polar field directions spontaneously assembled to create counter-balance with each other, leading to the formation of rice-like structures. The coupling process was on the basis of the polar field theory proposed by Jia et al. [25].

To clarify the role of the current density in experiments, the current densities were varied with the concentration of KCl being kept at 1 mmol/L. The SEM images of the resulting products are shown in Figure 5. The morphologies of ZnO products obtained in different current densities varied remarkably. In high current density (125 mA/cm^2), tubby rice-like ZnO particles (Figure 5a and b) were formed with an aspect ratio of 4.76 (average diameter of 1 μm and length of 210 nm). Two cones at the ends were dominated in the ZnO particles. When the current density decreased to 51.7 mA/cm^2, uniform particles with rod-like morphologies were obtained. The aspect ratio increased to 6.with a length of 1.7 μm and a diameter of 280 nm. At the same time, the two cones at the ends became shorter (see Figure 5d). By further decreasing the current density to 20 mA/cm^2, the morphology of ZnO particles changed to elongated rod with a larger aspect ratio and no obvious cones at the ends (see Figure 5f). Figure 6a shows the dependence of the aspect ratios as a function of the current density. The best guess about the above controlling mechanism was that a higher current density was integrant for twin-cone architectures. Although the OA process of nanocrystals could be proceed via all crystal facets of the primary nanoparticles, the OA process along the c-axis may be preferred with the highest surface energy. At a lower current density, this OA preference in the c-axis would be more pronounced. Lower current intensity meant weaker OA driving forces, and thus the energy superiority of the [1000]-planes became more dominant. Thus the elongated rod-like ZnO particles will form. On the other hand, a higher current density drives the OA process perform in all crystal facets and thus the energy

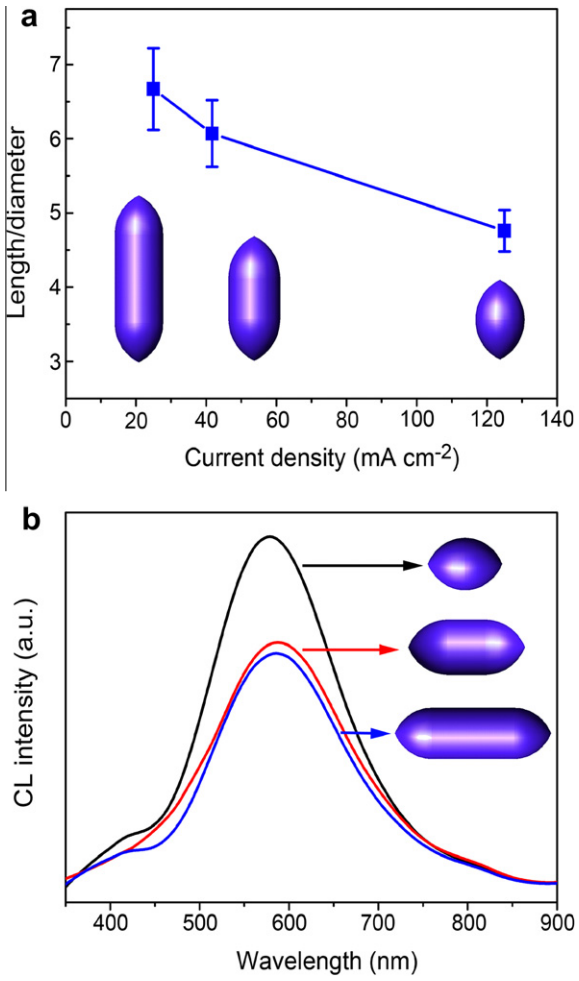

Figure 6. (a) Dependence of the aspect ratios (length to diameter) as a function of the current densities. Inset: schematic illustration of morphology evolution of ZnO particles with increasing current density. (b) CL spectra of ZnO particles with different morphologies grown at different current densities: 20, 51.7 and 125 mA/cm^2. Inset: morphologies of ZnO particles obtained in different currents densities.

superiority of the [1000]-planes will not stand out. The aspect ratio was significantly reduced and the growth of cone structure was facilitated. As a result, the morphology of the obtained ZnO particles changed to stubby rice-like shape with two obvious cones. This systematic correlation suggests that higher current density slowdown crystal growth along the preferred growth direction and therefore provides a simple approach to controlling the aspect ratio of ZnO mesocrystals.

To evaluate the luminescence qualities of the obtained ZnO products with different mophologies, CL measurement were carried out in room-temperature and the coresponding CL spectra are shown in Figure 6b. An obvious visible emission at about 575 nm is observed, while no UV emission is shown in the CL spectra. All the products show similar CL spectra features, except the absolute intensities. The ZnO particles obtained at a current density of 125 mA/cm^2 shows the strongest visible emission band, while the rod-like ZnO particles obtained at lower current densities show quite weaker visible emission. The significant difference of the visible luminescence might be explained in terms of irradiative defects, which were brought during the crystal growth processes. The visible emission is usually attributed to the complex of bound excition at the oxygen vacancies or interstitial Zn centers [26], which could be named as irradiative defects. The appearance of the visible emission indicated large density of irradiative defects may be generated at a certain current density condition. When the electrochemical deposition was carried out with the higher current density, the release rate of Zn^{2+} from the anode was higher, leading to the faster formation of ZnO particles. In this situation, more oxygen vacancies or interstitial Zn centers formed. Therefore, the emission is obviously enhanced. These results were similar to that proposed by Li et al. [27]. On the other hand, the UV emission corresponds to the near band gap transition and the recombination of free excitons [28]. As the ZnO building units were produced quickly during the electrochemical reaction, these ZnO building units attach together along with a certain of crystallographic orientation. However, a great number of imperfect attachment and insufficient fusion still exists. As a result, larger density of defects generated. A high defect density is usually an obstacle for emission or charge transport [29], which lead to the absence of UV emission. The existence and current density dependence of such zinc interstitial defects in the rice-like ZnO mesocrystals demands much in-depth work.

4. Conclusion

In summary, we have developed and systematically evaluated a facile electrochemical approach to synthesize a new class of well-defined ZnO mesocrystals. Results indicated that the rice-like ZnO possessed a single-crystal hexagonal wurtzite structure. Aside from the features in morphology and crystal structure, the ZnO particles have several unique characteristics. First, morphologies of these regular ZnO mesocrystals can be controllable tuned from tubby rice-like to elongated rod-like shape by change the electrochemical current densities. The aspect ratio of ZnO particles was significantly decreased with the increase of the current density, revealing that higher current densities appear to be critical to the formation of the cone structure. Second, a detailed study revealed a special crystallization process that single cone was formed in the 'OA' manner and served as the base for final twin-cone structure. The following smooth process of the crystal surface was in the 'OR' manner. Third, room-temperature CL spectra indicate that the ZnO mesocrystals exhibit an obvious visible emission and no UV emission is observed. The CL emission is remarkably enhanced with an increase of the irradiative defect in the particle, which is associated with the quick growth driven by high deposition current. The absence of UV emission indicates that the ZnO mesocrystals are composed of a large density of defects, demonstrating one of the unique structural characteristics of mesocrystals. This Letter provides a new easy route to prepare ZnO mesocrystals without use any template, surfactant or severe reaction conditions, such as high temperature and high vacuum. The feasibility of the present facile approach toward size-controllable production of ZnO mesocrystals shall foster further interest to investigate their practical applications in some versatile applications, such as Humidity sensing.

Acknowledgments

J.X. Fang was supported by National Natural Science Foundation of China (Nos. 51171139 and 50901056), Tengfei Talent Project of Xi'an Jiaotong University, the New Century Excellent Talents in University (NCET), Doctoral Fund for New Teachers (No. 20110201120039), the Fundamental Research Funds for the Central Universities (No. 08142008) and Scientific New Star Program in Shann Xi Provience (No.2012KJXX-03). H.J. You was supported by National Natural Science Foundation of China (No. 51201122), and Natural Science Foundation of Shaanxi Province (No. 2012JQ6006).

References

[1] R.Q. Song, H. Cölfen, Adv. Mater. 22 (2010) 1301.
[2] T.X. Wang, H. Cölfen, M. Antonietti, J. Am. Chem. Soc. 127 (2005) 3246.
[3] X. Fang, B.J. Ding, X.P. Song, Y. Han, Appl. Phys. Lett. 92 (2008) 173120.
[4] J.X. Fang, B.J. Ding, X.P. Song, Cryst. Growth Des. 8 (2008) 3616.
[5] L.C. Soare, P. Bowen, J. Lemaitre, H.J. Hofmann, J. Phys. Chem. B 110 (2006) 17763.
[6] C. Zhang, J. Chen, Y.C. Zhou, D.Q. Li, J. Phys. Chem. C 112 (2008) 100.
[7] J.X. Fang, B.J. Ding, H. Gleiter, Chem. Soc. Rev. 40 (2011) 5347.
[8] Z.R. Tian et al., Nat. Mater. 2 (2003) 821.
[9] Z.W. Pan, Z.R. Dai, Z.L. Wang, Science 291 (2001) 1947.
[10] B. Liu, H.C. Zeng, J. Am. Chem. Soc. 126 (2004) 16744.
[11] M.H. Huang et al., Science 292 (2001) 1897.
[12] B. Liu, H.C. Zeng, J. Am. Chem. Soc. 125 (2003) 4430.
[13] F. Meng, J. Yin, Y.Q. Duan, Z.H. Yuan, L.J. Bie, Sens. Actuators, B 156 (2011) 703.
[14] H. Zhang, D.R. yang, X.Y. Ma, Y.J. Ji, J. Xu, D. Que, Nanotechnology 15 (2004) 622.
[15] F.F. Wang et al., J. Phys. Chem. C 111 (2007) 7655.
[16] C. Ristoscu, M. Socol, G. Socol, I.N. Mihailescu, R. Jafer, Y. Al-Hadeethi, D. Batani, Appl. Phys. A 104 (2011) 871.
[17] M. Distaso, R.N.K. Taylor, N. Taccardi, P. Wasserscheid, W. Peukert, Chem. Eur. J. 17 (2011) 2923.
[18] M. Distaso, D. Segets, R. Wernet, R. Klupp, T.W. Peukert, Nanoscale 4 (2012) 864.
[19] J.X. Fang, H.J. You, P. Kong, B.J. Ding, X.P. Song, Appl. Phys. Lett. 92 (2008) 143111.
[20] H.L. Cao, X.F. Qian, Q. Gong, W.M. Du, X.D. Ma, Z.K. Zhu, Nanotechnology 17 (2006) 3632.
[21] R. Viswanatha, P.K. Santra, C. Dasgupta, D.D. Sarma, Phys. Rev. Lett. 98 (2007) 255501.
[22] H.M. Luo, J.F. Zhang, Y.S. Yan, Chem. Mater. 15 (2003) 3769.
[23] J.Y. Dong, W.H. Lin, Y.J. Hsu, D.S.H. Wong, S.Y. Lu, CrystEngComm 13 (2011) 6218.
[24] J.Y. Dong, Y.J. Hsu, D.S.H. Wong, S.Y. Lu, J. Phys. Chem. C 114 (2010) 8867.
[25] L.C. Jia, W.P. Cai, H.Q. Wang, H.B. Zeng, Cryst. Growth Des. 8 (2008) 4367.
[26] K. Vanheusden, C.H. Seager, D.R. Tallant, J.A. Voigt, B.E. Gnade, W.L. Warren, J. Appl. Phys. 79 (1996) 7983.
[27] G.R. Li et al., J. Phys. Chem. C 111 (2007) 1919.
[28] S.C. Lyu, Y. Zhang, H. Ruh, H.J. Lee, H.W. Shim, E.K. Suh, C.J. Lee, Chem. Phys. Lett. 363 (2002) 134.
[29] G. Teyssedre, C. Laurent, IEEE Trans. Dielectr. Electr. Insul. 12 (2005) 857.